P-V-M Interaction Curves for Seismic Design of Steel Column Base Connections

JASWANT N. ARLEKAR and C.V.R. MURTY

ABSTRACT

Recent studies on connections have shown that the beam bending theory cannot predict the flow of forces near the connection regions. In this paper, a new truss analogy model has been proposed to better represent the flow of forces near the column base connections. Also, shear-moment strength envelopes, generated for different levels of axial load using the hysteretic stress-strain curves for steel, are presented. The moment and shear demand for the design of column base connection elements are calculated using the normalized *P-V-M* interaction curves. Appropriate strength factors applied to the moment capacity of the column section to account for the uncertainty in the estimation of yield stress, strain hardening, compactness of the section, and slenderness of the member are discussed. Finally, a generalized procedure for the capacity design of column base connections is proposed.

INTRODUCTION

Column base connections play a critical role in the seismic performance of steel moment resisting frame (MRF) buildings. Failure of column base connections can lead to an undesirable brittle response and even collapse of the structure. Following the hierarchy of members of a building as enlisted by the Capacity Design Concept (Penelis and Kappos, 1997), (a) the column has to be stronger than the beam, (b) the beam-to-column joint stronger than the beam, and (c) column base connections stronger than the column.

Traditional column base design procedures address only the design of a column base plate from the point of view of distribution of the forces to the foundation block under it. The base plate is welded to the column with nominal stiffeners only around the anchoring bolts (Englekirk, 1994). It is assumed that the column forces are transferred to the base plate as per the beam bending theory, i.e., the shear is transferred through the web and the bending moment through the flanges. However, recent research has shown that the classical beam bending theory cannot be used to represent the flow of forces near the connection region (e.g., Goel, Stojadinovic, and Lee, 1996; Fahmy, Stojadinovic, Goel, and Sokol, 1998). The restraint provided by the column base plate to the column is similar to the restraint provided by the column to the beam in the case of beam-to-column connections. This restraint does not allow the ductile yielding of the column near the base plate (Miller, 1998). To have the desired ductile yielding of the column base, it is essential to avoid the premature fracture of welds there. In the present study, a comprehensive procedure is proposed for the design of column base connection based on the Capacity Design Concept. Design of column base connections by this procedure will ensure ductile yielding of the column in the event of extreme seismic shaking.

Jaswant N. Arlekar is Ph.D. student, department of civil engineering, Indian Institute of Technology, Kanpur, India.

C.V.R. Murty is associate professor, department of civil engineering, Indian Institute of Technology, Kanpur, India.

HYSTERETIC AXIAL LOAD-SHEAR-MOMENT (*P-V-M*) INTERACTION

The axial force-moment (*P-M*) interaction curves for steel wide flange sections currently used in design do not consider the hysteretic behavior of the material. For instance, while obtaining the M-φ curves, the strain profile resulting from the simultaneous application of axial load (P) and a specific curvature φ is imposed on the section in one step starting with zero initial curvature and zero initial axial strain, irrespective of the state of the section at the immediately preceding curvature value; the stresses in the fibers are obtained directly from the virgin stress-strain curve.

In this study, a fiber model is used to develop the *V-M* interaction curves for sections subjected to known compressive axial loads. Due to the presence of the axial load, the section is already subjected to some initial axial strain. Now, if this section is subjected to a specific curvature, φ, to keep the axial load, P, constant, the axial strain in the section also changes if the section goes into inelasticity. The strain-hardened stress-strain curve of steel with the rules for hysteretic behavior used in this study is graphically shown in Figure 1. A stressed fiber returns along the virgin stress-strain curve only within the initial elastic range. Fibers that are subjected to increased axial strain will continue along the virgin stress-strain curve, and those subjected to reduced strain will return along (a) the virgin stress-strain curve if the fiber is in the elastic range, or (b) the new unloading stress-strain curve, which is parallel to the initial elastic portion of the virgin stress-strain curve if the fiber is in the inelastic range. Thus, for fibers already beyond the elastic limit, unloading takes place along a new unloading curve.

On further unloading, some fibers may reach the translated virgin stress-strain curve in the other direction, and from then on they follow the same path.

To generate the shear-moment (*V-M*) interaction curve corresponding to a certain axial load P, first the strain in the fibers is obtained for that level of axial load. The curvature on the column section is incrementally increased over the already existing strain profile. If inelasticity exists at the curvature increment, then the axial strain is also increased in small steps until the resultant axial force is equal to the applied axial load. Once the strain profile is such that the resultant of normal stresses is equal to the applied axial load, the stresses in the fibers are updated ensuring that their loading, unloading or reloading is in accordance with the hysteretic rules depicted in Figure 1. Thus, the stress profile at any section for a given curvature is dependent on the state of stress at the end of the immediately preceding curvature increment. The next level of curvature increment is applied to this updated state of the fibers.

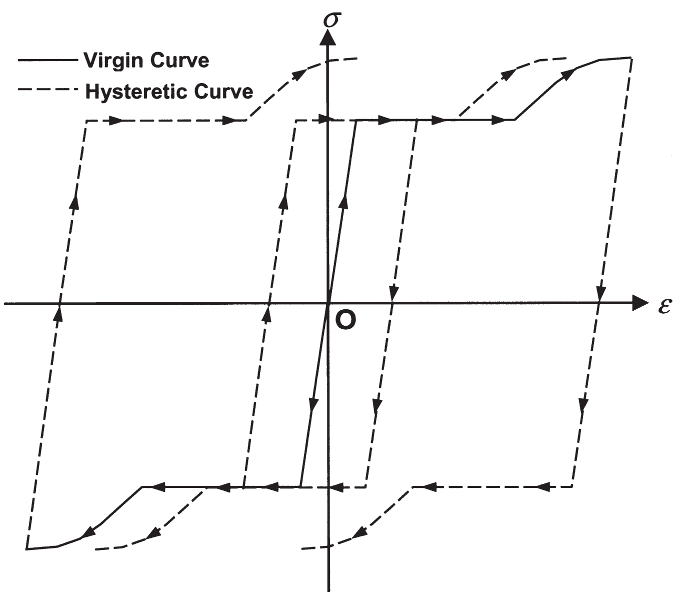

Fig. 1. Schematic representation of the loading and unloading paths for steel.

Normalized *V-M* interaction curves for a typical AISC section (W21×142) for various levels of the compressive axial load are obtained as discussed above (Figure 2). The moment is normalized with the nominal plastic moment capacity $M_p(= F_yZ_c)$ and shear with the nominal shear capacity $V_p(= \tau_y t_{cw} d_c)$. The *V-M* interaction curves obtained using a strain-hardened initial stress-strain curve are also shown in Figure 2. The *V-M* curves without hysteretic loading are marginally higher than the corresponding curves obtained using the hysteretic loading, only when the axial load is higher than P_y (Figure 2). Figure 3 shows the three-dimensional hysteretic *P-V-M* surface for W21×142. This surface consists of two distinct portions demarcated by $P = P_y$. The idealization of the *P-V-M* surface for the two regions is discussed below.

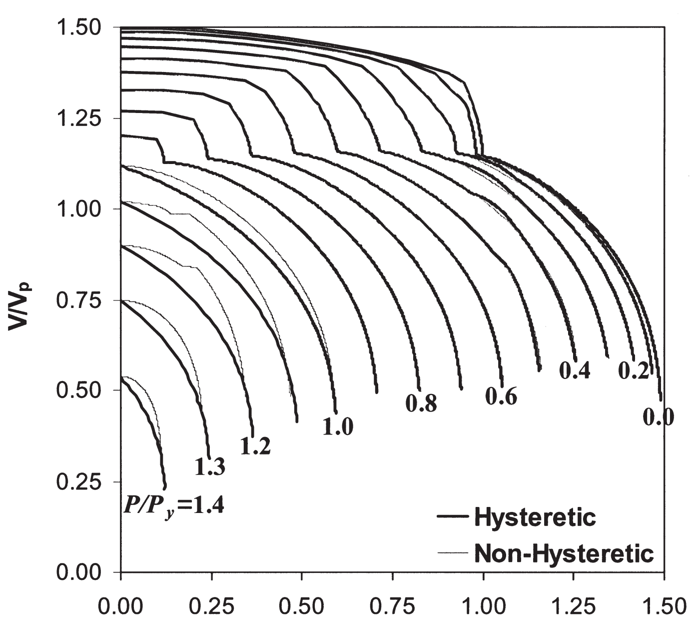

Fig. 2. Normalized V-M curves for a typical AISC section (W21×142) with and without hysteretic stress-strain curve.

Axial Load—Shear (*P-V*) Interaction for Zero Moment

The Von Mises criterion for ultimate strength of steel is represented by

$$\left(\frac{\sigma_{xx}}{F_y}\right)^2 + \left(\frac{\tau_{xz}}{F_y/\sqrt{3}}\right)^2 = \left(\frac{F_u}{F_y}\right)^2 \tag{1}$$

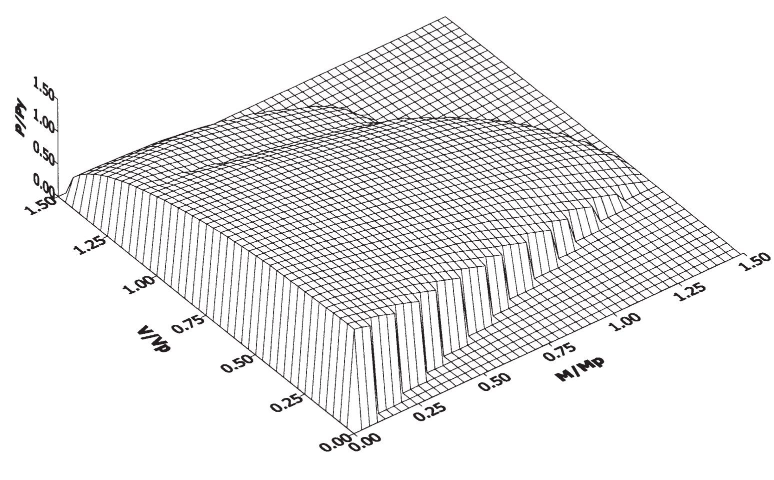

Fig. 3. Normalized P-V-M surface using hysteretic stress-strain curve for a typical AISC section (W21×142).

where σ_{xx}, τ_{xz} and F_y are the normal, shear and yield stress, respectively. F_u/F_y is the ratio of ultimate stress to the yield stress for steel, and is assumed to be 1.5 in this study. Using the definitions, $P_y = AF_y$ and $V_p = A_w\left(F_y/\sqrt{3}\right)$, where A and A_w are the areas of the section and the web, respectively, Equation 1 can be expressed as

$$\left(\frac{P}{P_y}\right)^2 + \left(\frac{V}{V_p}\right)^2 = \left(\frac{F_u}{F_y}\right)^2 \tag{2}$$

which is the equation of a circle of radius F_u/F_y. Here, P is the total axial load on the section and V is the corresponding shear capacity of the section. Thus, when the section is subjected to axial load and shear in the absence of moment, an ellipse can represent the *P-V* interaction.

Axial Load—Moment (*P-M*) Interaction for Zero Shear

The *P-M* interaction obtained in this study, using the fiber model with the hysteretic stress-strain curve for three AISC wide flange sections (d = 933 mm (W36×300), d = 545 mm (W21×142) and d = 289 mm (W12×58)) is shown in Figure 4. This figure also shows the bilinear P-M interaction curve, as prescribed by AISC (AISC, 1994), with maximum load capacity of the section as P_y. Since the normalized *P-V-M* surface obtained in this study is for the fully strain-hardened ultimate capacity, P_u, of the column, the AISC prescribed *P-M* curve is scaled to the ultimate capacity of the section. Clearly, the *P-M* interaction of AISC underestimates the capacity of the column; the actual *P-M* interaction points for the range of AISC sections considered in this study are outside the scaled AISC prescribed *P-M* interaction curve. Hence, the column base connections designed using the column capacities as per the AISC *P-M* interaction would be under-designed, particularly in high seismic regions. For a conservative design of the column base connections, any *P-M* interaction curve used for estimating the moment corresponding to a given level of axial load should be an outer bound envelope of the actual *P-M* interaction of the section. The following nonlinear *P-M* interaction curve for $V = 0$ is proposed as an outer bound (Figure 4):

$$\frac{P}{P_y} = \frac{F_u}{F_y}\left(1 - \frac{F_y}{F_u}\frac{M}{M_p}\right)^{0.7} \tag{3}$$

Idealization of *V-M* Curves

The *V-M* interaction curves obtained for different levels of axial loads for a typical section (W21×142) are shown in Figure 5. For the purpose of design, these curves are idealized using straight lines for $P \le P_y$. For $P > P_y$, these curves seem to be elliptical. However, these have not been idealized, as it is not desirable to design the columns such that they are subjected to axial loads larger then the yield load. The idealized *V-M* curves for $P \le P_y$ can be defined using four points, namely A, B, C and D, as shown in Figure 5. Point A, which is on the $V = 0$ axis, is defined by M for a given P using Equation 3. Similarly, point B, which is on the $M = 0$ axis, is defined by V for a given P using Equation 2. Point C is defined by

$$\frac{M_C}{M_p} = \frac{M_A}{M_p}, \qquad \frac{V_C}{V_p} = \frac{V_y}{V_p} \tag{4}$$

where $V_y = \frac{2}{3}V_p$, and point D is defined by

$$\frac{M_D}{M_p} = \frac{\left(V_B/V_p\right) - 1.085}{0.462}, \qquad \frac{V_D}{V_p} = \frac{V_B}{V_p} \tag{5}$$

Member Capacity Modification Factors

The *P-V-M* curves developed in this study are for the full capacity of the member without considering the effect of uncertainty in the estimation of yield strength, compactness

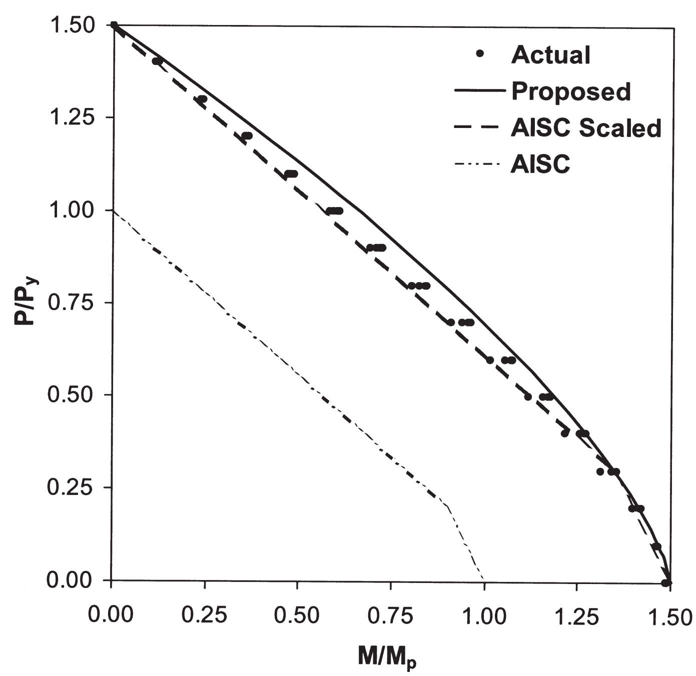

Fig. 4. Proposed P-M interaction curve along with the actual P-M points for V = 0, and the actual and scaled AISC P-M interaction curves [AISC, 1994].

of the section, slenderness of the member, and the stability against flexural-torsional buckling of the column. The first factor mentioned above is related to the strength of the member, and the latter three are related to the stability of the member. The effects of these factors and the method of incorporating them in the member capacity obtained from the *P-V-M* curves developed in this study are discussed below.

Yield Strength of Material

The P-V-M curves obtained in this study are for steel with yield strength of 250 MPa. However, coupon tests have shown that the actual yield strength can be higher than the minimum specified yield strength (Malley and Frank, 2000). The AISC *Seismic Provisions for Structural Steel Buildings* (SPSSB) (AISC, 1997) recommend the use of higher yield strength while calculating the member strength for the determination of the design forces for connection elements (AISC, 1997); the ratio R_y of the expected yield strength to the minimum specified yield strength of the connected member as suggested by AISC (AISC, 1997) varies from 1.1 to 1.3 for different grades of steel.

Strain-Hardening of Material

The deformations at the column base are expected to be such that a portion of the member section can strain-harden. However it is very unlikely that the member will achieve its full strain-hardened capacity. FEMA recommends a value of 1.2 for the strain-hardening factor while designing the

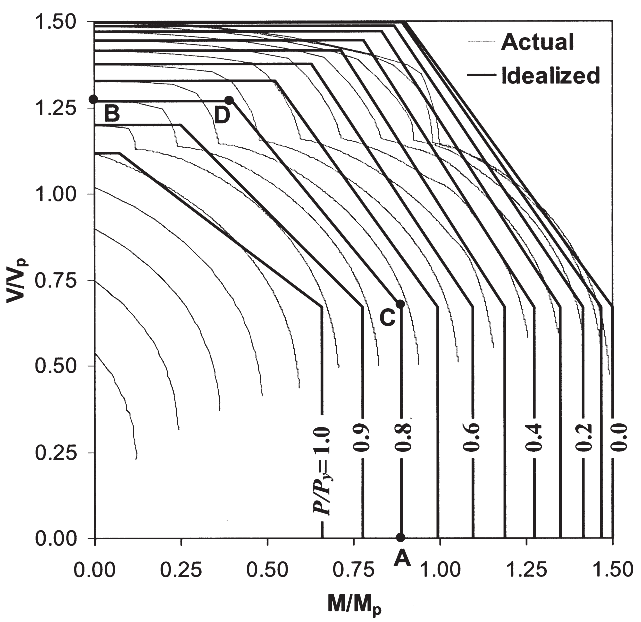

Fig. 5. V-M curves with the idealized curves for a typical section (W21×142).

beam-to-column connections (FEMA, 1995). In a study for the design of MRF beam-to-column connections, it was shown that for the level of deformation expected in beams, the strain-hardening factor ranges from 1.0 to 1.28 (Arlekar, 2002). The *V-M* curves developed in this study are based on the strain-hardening stress-strain curve for steel. Thus, the use of these curves for calculating the maximum member capacities includes the effect of strain-hardening.

Compactness of Section

Local buckling of the flanges and web of the column can adversely affect its maximum strength. It is unlikely that a noncompact section will develop its full capacity. Thus, designing the column base connection for the full section capacity can be uneconomical. The AISC-LRFD provisions (AISC, 1994) help in assessing the local stability of the column. According to the AISC compactness provisions, the section is compact if *b/t* is less than λ_p, slender if *b/t* ratio is more than λ_r, and noncompact if *b/t* ratio is between λ_p and λ_r, where λ_p is the limiting slenderness parameter for a compact section and λ_r is the limiting slenderness parameter for a noncompact section, as defined in AISC-LRFD (AISC, 1994). Thus, if the *b/t* ratio classifies the section to be slender, then the member buckles locally, prior to reaching its maximum capacity. Since the column capacity, *M*, as determined from the *P-V-M* interaction does not consider the effect of the compactness of the section, a compactness factor, R_c, is introduced to account for the reduction in the maximum achievable member capacity owing to premature local buckling, where

$$R_c = \begin{cases} 1.0 & \text{for } \dfrac{b}{t} \le \lambda_p \\ 1.0 - 0.2\left\{\dfrac{(b/t) - \lambda_p}{\lambda_r - \lambda_p}\right\} & \text{for } \lambda_p < \dfrac{b}{t} \le \lambda_r \\ 0.8 & \text{for } \dfrac{b}{t} > \lambda_r \end{cases} \qquad (6)$$

As seen from the expression (Equation 6), the minimum value of R_c is 0.8.

Slenderness of Member

The global buckling of the column under compressive loads also reduces its maximum capacity. Again, the *P-V-M* interaction curves obtained for different levels of axial loads do not consider the effect of the slenderness of the column. Thus, the capacity of the member for the calculation of the column base connection design forces, as obtained from the idealized *P-V-M* curves, has to be modified to reflect the effect of global slenderness of the member. The global slenderness parameter, λ_c, as defined in AISC-LRFD (AISC, 1994) is used to reduce the member capacity, where

$$R_\lambda = \begin{cases} 0.658^{\lambda_c^2} & \text{for } \lambda_c \le 1.5 \\ \dfrac{0.877}{\lambda_c^2} & \text{for } \lambda_c > 1.5 \end{cases} \tag{7}$$

To qualify as a compact section that is capable of attaining post-yield strains, the column slenderness is limited by $l/r = 2.2\sqrt{E/F_y}$ (Englekirk, 1994), which corresponds to $\lambda_c = 0.7$ and $R_\lambda = 0.82$ for $F_y = 250$ MPa.

Flexural-Torsional Buckling of Member

Flexural-torsional buckling is yet another mode of failure whose influence can be considered in the design of column-base connections. AISC-LRFD (AISC, 1994) accounts for this mode of failure by reducing the critical design stress for the member. The flexural-torsional member capacity modification factor, using the AISC-LRFD provision is given by

$$R_L = \left[\frac{\pi^2 E C_w}{K_z l} + GJ\right]\frac{1}{\left(I_x + I_y\right)F_y} \text{ with a maximum of 1.0} \tag{8}$$

where

C_w = the warping constant
K_z = the effective length factor for torsional buckling
l = the length of the member
G = the shear modulus
J = the torsional constant
I_x, I_y = the moment of inertia about the x and y axes, respectively (AISC, 1994)

For the W-sections used in this study, flexural-torsional buckling is not the first mode of failure; R_L values calculated from Equation 8 are greater than 1.0 for $K_z = 1.0$ and $l = 3.8$ m, and hence R_L may be taken as 1.0.

Moment Capacity of Member

The strength modification factors (R_y and strain hardening) are independent of each other and are applied to the maximum member capacity. While considering the effect of the stability factors (R_c, R_λ, and R_L) on the member capacity for the design of connections, the factor corresponding to the first mode of instability is considered. Considering the modification factors discussed above, the maximum probable moment capacity M_{pr}^P (for full strain-hardening) of the column is given by

$$\frac{M_{pr}^P}{M_p^P} = R = R_y Min\left[R_c ; R_\lambda ; R_L\right] \tag{9}$$

where

R = the overall member capacity factor
M_{pr}^P = the full moment capacity of the section subjected to an axial load of P calculated using Equation 3

COLUMN BASE CONNECTION DESIGN

The P-M interaction is symmetric about the V-M plane at $P = 0$, with the maximum moment $M/M_p = F_u/F_y$ occurring at $P = 0$. Thus, the worst case for column base connection design would be when $P = 0$. The moment on the connections reduces as the axial load in the column is increased either in tension or in compression. Prior to the earthquake, columns are always under axial compression. During strong shaking, if reversal of axial load takes place, the column has to go through the load level $P = 0$. Thus, in such cases, it is proposed that the column base connections be designed for the moment and shear capacity of the column corresponding to $P = 0$.

Determination of Axial Load (P) for Column Base Design

The presence of axial load in the column reduces its capacity. But, sometimes, particularly in low seismic regions, designing the column base connections for moment and shear capacity of the column corresponding to $P = 0$ may be too conservative. Since the column base connections are to be designed to resist the shear and moment capacities of the column corresponding to the axial load in the column, this axial load in the column has to be determined. Keeping in mind that the design earthquake forces Q_E are only a fraction of the actual load appearing on the structure during the earthquake, the maximum forces on the structure during strong earthquake shaking may be obtained from the following load combination prescribed by AISC (AISC, 1997),

$$1.2DL + 0.5LL + \Omega_o Q_E \tag{10}$$

$$0.9DL - \Omega_o Q_E \tag{11}$$

where

DL and LL = the dead and live loads, respectively
Ω_o = the overstrength factor of the building

A column, in its initial condition, is always under compression. During the ground shaking it is possible that the column may be subjected to tension. If according to these combinations, the column can go into tension, then it has to pass the $P = 0$ condition (Figures 5 and 6). Further, the P-V-M interaction is symmetric about the $P = 0$ plane indicating that the most critical loading condition exists when the axial load is zero. Thus, the column base connection for a column under tension should be designed for the shear and moment capacities of the column corresponding to $P = 0$. Otherwise, the connection will be designed for shear and moment capacities of the column corresponding to the lowest compressive axial load. For a column subjected to tension or uplift, anchor bolts with adequate capacity should be provided. The maximum tension and moment for the design of the anchor bolts should be obtained from load combinations given in Equation 10 and 11.

If the building is designed according to the strong-column weak-beam (SCWB) philosophy, during extreme seismic shaking, plastic hinges will form in the beams and not in the columns. And, according to the capacity design approach, the column base should be stronger than the column itself. Thus, the worst scenario should be considered for the design of the column base, which corresponds to the case when the building forms a mechanism. Figure 6(a) shows a sketch of a typical ground story exterior column with the connection elements for the column base and the beam-to-column connection. The two possible mechanisms, namely a sway mechanism and a story mechanism, are shown in Figures 6(b) and 6(c), respectively. In Mechanism I (Figure 6(b)), the *sway mechanism*, plastic hinges are located at the beam-ends and at the base of the column in the ground story. In Mechanism II (Figure 6(c)), the *story mechanism*, plastic hinges are located at the top and bottom of the ground story column. Due to the presence of the reinforcement plates of the beam-to-column connection at the top, and of the column base connection at the base of the column, plastic hinges will be located at a distance l_t from the end of the connection reinforcement region. The length H_{o1} of the shear-link for Mechanism I, assuming that the moment at the column base is maximum, is given by

$$H_{o1} = H - (l_t + h_{cc}) \tag{12}$$

and the length H_{o2} for Mechanism II, considering that the column is bent in reverse curvature with maximum moments occurring at both the top and bottom of the column, is given by

$$H_{o2} = H - \left(\frac{d_b}{2} + h_{cb} + l_t + l_t + h_{cc}\right) \tag{13}$$

where

H = the story height

d_b, d_c = the depths of beam and column sections, respectively

h_{cb}, h_{cc} = the heights of the connection reinforcement regions at the top and bottom of the column, respectively

The shear and moment on the column base connection for Mechanism I are related by

$$\frac{V_1}{M} = \frac{1}{H_{o1}} \tag{14}$$

and for Mechanism II, by

$$\frac{V_2}{M} = \frac{2}{H_{o2}} \tag{15}$$

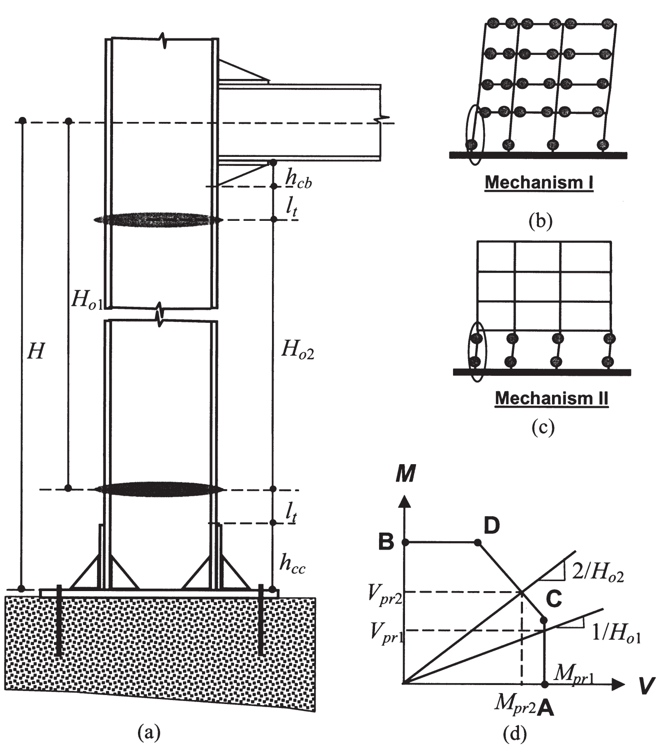

Fig. 6. (a) Details of a ground story exterior column showing the positions of beam connections and column base connections, (b) Collapse Mechanism I—sway mechanism, (c) Collapse Mechanism II—story mechanism, and (d) Column moment-shear plots for the possible collapse mechanisms.

From Figure 6(d), the connection design shear force for Mechanism I is lower than that for Mechanism II, but the moment is higher in the latter. If the building is designed by the SCWB philosophy, the sway collapse mechanism is more likely. However, in buildings with open ground stories and infills in the upper stories, the possibility of the story collapse mechanism occurring cannot be ruled out. Thus, it is essential to ensure that the column base connection is able to resist the forces resulting from each of these mechanisms.

The design of column-base connection in this study is applicable for any degree of foundation flexibility. The flexibility of foundation, if any, should be incorporated during the global analysis of the structure. Design of connections based on forces for rigid foundation considerations results in the upper bound of the design forces for the connection elements.

Truss Model for Calculation of Column Base Connection Forces

An earlier detailed finite element study of a column base connection with a base plate showed that a strut-and-tie

Table 1. Location of Truss Point for the Different Column Bases Considered in this Study

W-Section (1)	d_c (mm) (2)	P_y (kN) (3)	V_p (kN) (4)	P_y/V_p (5)	l_t (mm) (6)	l_t/d_c (7)
W36×300	933	14177	3247	4.37	393	0.421
W33×240	851	11344	2591	4.38	339	0.417
W27×177	694	8223	1811	5.54	312	0.450
W21×142	545	6754	1343	5.03	289	0.512
W18×114	469	5334	1020	5.23	200	0.427
W16×96	415	4533	842	5.38	187	0.451
W14×84	360	3930	574	6.84	179	0.497
W12×58	310	2658	405	6.57	146	0.471

model could be used to represent the flow of forces near the column base (Fahmy et al., 1998). However, in that study, the column was connected to the base plate directly without any connecting elements; a 60° truss model starting at the column-to-base plate interface was suggested to represent the flow of forces in the column base region. The study also reported that for this arrangement, the deformations near the base plate result in high stress concentrations at the interface of the column flanges and the base plate. The restraint provided by the base plate in combination with the high stress concentration may lead to premature fracture of the welds at the junction between the column and the base plate. To avoid the premature brittle fracture of the welds between the column and the base plate, the deformation demands on the welds there have to be reduced. This can be achieved by reinforcing this region using flange cover plates and rib plates. This reinforcement reduces the stress levels and the deformation demands on the welds by shifting the plastic hinge into the column.

Recent studies have shown that the truss analogy model can be used to better represent the flow of forces near the beam-to-column connection region (Goel et al, 1996; Lee, Goel, and Stojadinovic, 2000). In another study for beam-to-column connection design (Arlekar and Murty, 2000), the dimension of the equivalent truss end panel l_t was given in terms of the depth d_b of the beam, as

$$\frac{l_t}{d_b} = 0.5 \tag{16}$$

Here, l_t is the distance of the truss point from the end of the connection reinforcement region. In the beam-to-column connection design, the location of truss point determines the moment amplification due to shear. The larger the l_t, the higher is the amplification.

During lateral seismic shaking, the column base is subjected to combined moment, shear and axial force. The presence of axial load (P) in addition to moment (M) and shear (V) increases the stress intensity on the column sections. Thus, the normal stress intensity increases for sections closer to the column base (Figure 7a). Also, due to the end effects, the shear stresses near the column base connection are such that they increase the Von Mises stress near the flanges of the column (Lee et al., 2000). The resultant of normal and shear stress leads to the shifting of the plastic moment hinge towards the column base. Due to the presence of moment, M, and the axial load, P, the fibers of the section are subjected to normal stresses, whereas due to the presence of shear, V, they are subjected to horizontal shearing stresses. Thus, the stresses due to M and P are different from those due to V. During extreme seismic shaking, both P and M on the section are large and varying. The resultant axial load due to M and P may be shifted towards the compression flange of the column; an extreme case would be when the resultant compressive force is located in the compression flange itself. The load eccentricity, e, associated with strain-hardened moment, $C_{pr}M_p$, and axial yield load, P_y, is given by

$$e = \frac{d}{2}\left[4s\left(\frac{r}{d}\right)^2\right] \tag{17}$$

where

s = the shape factor of the cross section

r = the radius of gyration

d = the depth of the section

For the W-sections considered in this study, e varies from 0.94 to 1.0 times $d/2$. Thus, considering P to act along the flange of the column seems reasonable.

In this study, finite element analyses of 8 different column base connections have been carried out to identify the location of the truss point for the flow forces near the column base connection. The length of column is assumed to be 3.8 m and only the symmetric half of the column is modeled with the column base; the compressive axial load and the shear force applied at the mid-height of the column are equal to P_y and V_y, respectively (Figure 7a). The arrangement of column base reinforcing elements adopted in this study is shown in Figure 7(a). Figure 7(b) shows the finite element mesh of the half model. Due to the non-uniform distribution of stresses along the depth of the column section, the plastic hinge will be initiated in the compression flange of the column. It is suggested that this point of initiation of the plastic hinge be taken as the truss point (Arlekar and Murty, 2000). Thus, the first point in the web of the column beyond the column base connection reinforcement region, at which the shear stress is largest, is the truss point. Table 1 shows the location of the truss points for the 8 different column base connections analyzed in this study. The upper bound for the ratios of the truss length l_t to the depth of the column d_c is given by

$$\frac{l_t}{d_c} = 0.5 \tag{18}$$

Based on the observations of the above finite element analyses, two different trusses are used to represent the flow of forces near the connection region; one for the normal forces (Figure 8(b)) and the other for the shear forces (Figure 8(c)). The resultant forces from the two truss models are shown in Figure 8(d). The truss model is based on the assumption that the plastic hinge is located at a distance of $0.5d_c$ from the end of the column base connection reinforcement region. The design shear, V_{pd}, is calculated based on the failure mechanism under consideration. The vertical, P_{pd}, and horizontal, H_{pd}, design forces for the design of column base connections are

$$P_{pd} = \frac{M_{pd}}{d_c} + \frac{V_{pd}}{2} + \frac{P}{A}\left(A_f + \frac{A_w}{2}\right), \text{ and} \tag{19}$$

$$H_{pd} = \frac{V_{pd}}{2} \tag{20}$$

where A, A_f and A_w are area of the column section, area of column flange, and area of column web, respectively. The truss model for the transfer of M and P is shown in Figure 8(b). In this figure, P_f is the axial load shared by the column flanges and is expressed as

$$P_f = P\frac{A_f}{A} \tag{21}$$

Similarly, P_w is the axial load shared by the column web and is expressed as

$$P_w = P\frac{A_w}{A} \tag{22}$$

For the transfer of shear, it is assumed that the truss point is located at a distance of $0.5d_c$ from the end of connection reinforcement region; the truss model for the transfer of shear is shown in Figure 8(c). In Figure 8 (b), (c) and (d), the signs of various terms are consistent with the directions of the force resultants shown.

CAPACITY DESIGN PROCEDURE FOR COLUMN BASE CONNECTIONS

A connection configuration consisting of outer flange cover plates and vertical (inner and outer) rib plates is used in this study (Figure 7). The column and the connection elements are welded to the base plate using complete-joint-penetration groove welds. The column flange cover plates are welded to the column flanges through fillet welds as shown in Figure 7(a). Fillet welds are used between the connection elements and the column. The recommended mode of failure or distress for the column base is the failure of the column due to instability or the formation of a plastic hinge near the column base. This study does not consider the design of the column base plate and anchor bolts, and it is recommended that these should be designed ensuring adequate strength so that they do not fail before the failure of the column. The procedure for the strength design of base plates and anchors is already available (DeWolf and Ricker, 1990). The following step-wise procedure is suggested for the design of column base connections.

Part A: Capacity Reduction Factors and Axial Load

1. Estimate the material yield strength uncertainty factor, R_y, from field data. In case of unavailable data, the R_y factor of AISC-SPSSB (AISC, 1997) may be used.
2. Determine the compactness factor, R_c, the slenderness factor, R_λ, and the flexural-torsional factor, R_L, using Equation 6, Equation 7 and Equation 8, respectively.

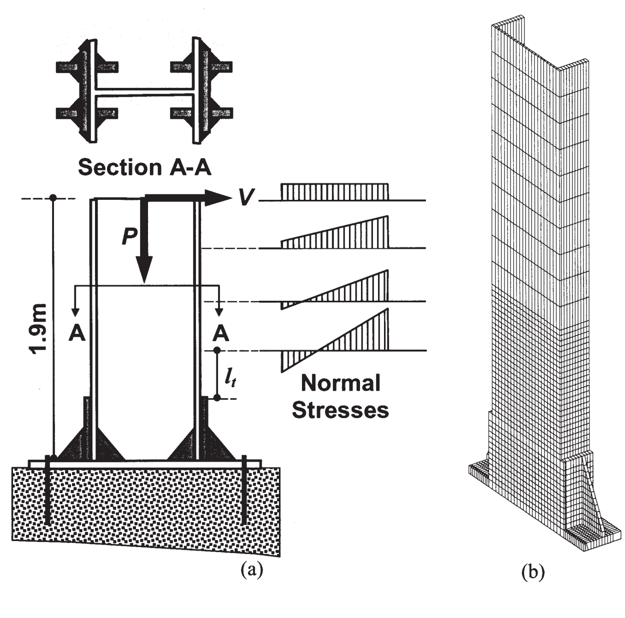

Fig. 7. (a) Column base sub-assemblage analyzed in this study with the distribution of normal stress (elastic) along the depth of the column, and (b) Finite element mesh of the symmetric half of the column base sub-assemblage.

3. Determine the minimum level of axial load in the column from the elastic analysis of the structure using the load combinations given in Equation 10 and Equation 11. If the axial load is tensile, set it to $P = 0$.
4. Identify the *V-M* curve for this level of axial load by following the procedure described in the section on idealization of *V-M* curves.

Part B: Dimensions of Cover Plates

5. Assume the thickness, t_{cp}, of the vertical flange cover plate. This should be close to the thickness of the column flange.
6. Assume the width, b_{cp}, of the flange cover plate.

Part C: Shear and Moment Demand on Connection

7. Calculate the yield capacity of column flange using

$$T_{cf} = F_y b_{cf} t_{cf} \tag{23}$$

8. Calculate the yield capacity of flange cover plate using

$$T_{cp} = F_y b_{cp} t_{cp} \tag{24}$$

9. Calculate the length of the fillet weld between the column flange and the flange cover plate, using

$$l_{wcp} = \frac{T_{cp}}{\dfrac{F_y}{\sqrt{3}} \dfrac{t_{wcp}}{\sqrt{2}}} \tag{25}$$

where t_{wcp} is the size of the fillet weld between the column flange and cover plate.

10. The length, l_{wcp} is contributed by the fillet welds between the cover plate and the column flange. Thus, there are 2 weld lines of equal size in total (Figure 7(a)). Calculate the length, l_c, of the cover plate as

$$l_c = \frac{l_{wcp} - Min\left[b_{cp}; b_{cf}\right]}{2} \tag{26}$$

11. Calculate the shear link lengths, H_{o1} and H_{o2}, for the two failure mechanisms assuming that plastic hinges are located at a distance of $0.5d_c$ from the end of the connection reinforcement region (Figure 8(a)), using Equation 12 and Equation 13.
12. Calculate the probable maximum shear force, V_{pr}, corresponding to the sway collapse mechanism using Equation 14.
13. Obtain the capacity moment, M_{pr}, corresponding to V_{pr} from the *V-M* interaction curves (Equation 4 and Equation 5, and Figure 5) for the appropriate level of axial load.
14. Calculate the design moment and design shear for the column base connection, using

$$M_{pd} = RM_{pr} \tag{27}$$

$$\text{and } V_{pd} = RV_{pr} \tag{28}$$

Part D: Dimensions of Vertical Rib Plate

15. Calculate the maximum horizontal and vertical forces for which the half portion of the connection will be designed using Equation 19 and Equation 20.
16. Calculate the design forces in the rib plate, namely the vertical axial pull force, P_{rp}, and the horizontal shear force, H_{rp}, using

$$P_{rp} = \frac{P_{pd} - T_{cp} - T_{cf}}{4} \tag{29}$$

$$\text{and } H_{rp} = \frac{H_{pd}}{4} \tag{30}$$

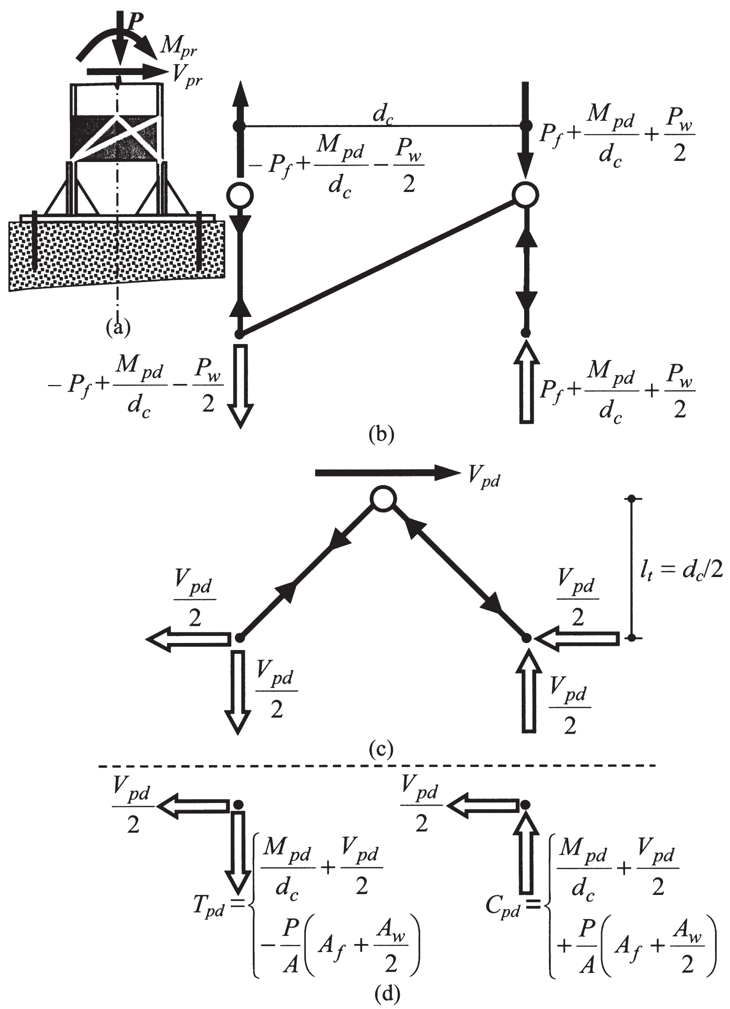

Fig. 8. (a) Column base showing the location of truss model used for the calculation of the column base connection forces, (b) Configuration and geometry of the truss model for normal forces, (c) Configuration and geometry of truss model for shear force, and (d) Resultant forces of the truss model.

17. Calculate the area, A_{rp}, of the vertical rib plate for combined axial load and shear using Von Mises criterion

$$A_{rp} = \sqrt{\frac{P_{rp}^2 + 3H_{rp}^2}{F_y^2}} \tag{31}$$

Assume a thickness, t_{rp}, of the vertical rib plate close to the thickness of the cover plate, and calculate the width, b_{rp}, of the vertical rib plate from $b_{rp} = A_{rp}/t_{rp}$.

18. Calculate the length of the fillet weld between the rib plate and flange cover plate to transfer the vertical force of P_{rp} using

$$l_{wrp} = \frac{4P_{rp}}{\frac{F_y}{\sqrt{3}} \frac{t_{wrp}}{\sqrt{2}}} \tag{32}$$

where t_{wrp} is the size of the fillet weld, which is equal to the thickness of the rib plate. The height of the rib plate is $l_{wrp}/6$.

Part E: Check for Mechanism II and Moment Amplification

19. For the actual dimensions of the cover plate and vertical rib plates provided, calculate the capacities using

$$T_{cp}^* = F_y b_{cp} t_{cp} \tag{33}$$

$$T_{rp}^* = F_y h_{rp} t_{rp} \tag{34}$$

$$V_{rp}^* = \frac{F_y}{\sqrt{3}} h_{rp} t_{rp} \tag{35}$$

20. Ensure that the shear force corresponding to Mechanism II for the rib plate is less than the capacity of the rib plate using

$$\frac{V_2}{8} \le V_{rp}^* \tag{36}$$

This expression corresponds to the connection configuration used for illustration in this study, which has 8 rib-plates for shear transfer (Figure 7(a)). V_{rp}^* is the shear capacity for one rib plate as given in Equation 35.

21. Ensure that the connection moment capacity to resist the external moment is more than the moment demand on it including the effect of moment amplification, using

$$\left(4T_{rp}^* + T_{cp}^* + T_{cf}\right) d_c \ge M_{pd} + V_{pd}\left(l_c + \frac{d_c}{2}\right) \tag{37}$$

SUMMARY AND CONCLUDING REMARKS

Recent studies have shown that in high seismic zones, column bases without any reinforcing elements may not be sufficient to transfer the forces from the column to the foundation; such connection schemes may result in brittle failure of the column bases. A comprehensive procedure based on the *capacity design concept* is proposed for the design of column base connections. The maximum probable capacity of the column is estimated using the hysteretic *V-M* interaction curves generated in this study.

Detailed finite element analyses of eight different column base sub-assemblages are carried out to locate the point of initiation of the plastic hinge in the column. The results of these analyses are used to identify the truss model for the distribution of forces from the column to the column base connection elements. The column base connection elements (flange cover plates and the rib plates) are proportioned to transfer the axial load, bending moment and shear forces corresponding to the maximum probable capacity of the column.

ACKNOWLEDGMENT

The authors express their sincere appreciation to Ms. Shreya Mandrekar, for providing useful comments and improving the script of the paper.

REFERENCES

AISC (1994), *Metric Load and Resistant Factor Design Specification for Structural Steel Buildings*, American Institute of Steel Construction, Inc., Chicago, IL.

AISC (1997), *Seismic Provisions for Structural Steel Buildings*, American Institute of Steel Construction, Inc., Chicago, IL.

Arlekar, J.N. (2002), "Seismic Design of Strong-Axis Welded Connections in Steel Moment Resisting Frame Buildings," Ph.D. Thesis being submitted to Department of Civil Engineering, Indian Institute of Technology Kanpur, Kanpur, India.

Arlekar, J.N., and Murty, C.V.R. (2000), "Improved Truss Model for Design of Welded Steel MRF Connections," under review with *Journal of the Structural Division*, ASCE.

DeWolf, J.T. and Ricker, D.T. (1990), *Column Base Plates*, Steel Design Guide Series No. 1, American Institute of Steel Construction, Inc., Chicago, IL.

Englekirk, R. (1994), *Steel Structures: Controlling Behavior Through Design*, John Wiley & Sons, Inc., Singapore.

Fahmy, M.B., Stojadinovic, B., Goel, S.C., and Sokol, T. (1998), "Load Path and Deformation Mechanism for Moment Resisting Steel Column Bases," 6th U.S. National Conference on Earthquake Engineering, Seattle, WA.

FEMA (1995), "Interim Guidelines: Evaluation, Repair, Modification and Design of Welded Steel Moment Frame Structures," FEMA 267, Report No. SAC-95-02, SAC Joint Venture, CA.

Goel, S.C., Stojadinovic, B., and Lee, K.H. (1996), "A New Look at Steel Moment Connections," Report No. UMCEE 96-19, Department of Civil and Environmental Engineering, The University of Michigan, College of Engineering.

Lee, K.H., Goel, S.C., and Stojadinovic, B. (2000), "Boundary Effects in Steel Moment Connections," Paper No. 1098, 12th World Conference on Earthquake Engineering, Auckland, New Zealand.

Malley, J.O. and Frank, K. (2000) "Materials and Fracture Investigations in the FEMA/SAC PHASE 2 Steel Project," 12th World Conference on Earthquake Engineering, Paper ID. 2544, New Zealand.

Miller, D.K. (1998), "Lessons Learned from the Northridge Earthquake," *Engineering Structures*, Vol. 20, No. 4-6, pp. 249-260, Elsevier Science Ltd.

Penelis, G.G., and Kappos, A.J. (1997), *Earthquake—Resistant Concrete Structures*, E & FN Spon, Great Britain.

NOTATIONS

The following symbols are used in this paper:

A = Area of section
A_f = Area of flange
A_{rp} = Area of rib plate
A_w = Area of web
b = Width
b_{bf} = Width of beam flange
b_{cf} = Width of column flange
b_{cp} = Width of vertical flange cover plate
b_{rp} = Width of rib plate
C_{pr} = Factor to account for the strain-hardening of the section
C_w = Warping constant
DL = Dead load
d = Depth of section
d_b = Depth of beam section
d_c = Depth of column section
E = Modulus of elasticity
F_y = Minimum specified normal yield stress of steel
F_u = Ultimate normal stress
G = Shear Modulus
H_{o1} = Length of shear-link for failure Mechanism I
H_{o2} = Length of shear-link for failure Mechanism II
H_{pd} = Design horizontal force for column base connection
H_{rp} = Horizontal design shear force for the rib plate
h_{cb} = Height of connection reinforcement region at column top
h_{cc} = Height of connection reinforcement region at column base
I_x, I_y = Moment of inertia about principal axes
J = Torsional constant
K_z = Effective length factor for flexural-torsional buckling
LL = Live load
L,l = Length
l_c = Length of connection reinforcement region
l_t = Distance of the plastic hinge from the end of connection reinforcement end
l_{wcp} = Length of fillet weld between connection plates and column flange
l_{wrp} = Length of fillet weld between connection plates and rib plates
M = Bending moment
M_p = Section plastic moment capacity using minimum specified yield strength
M_{pd} = Connection design moment
M_p^P = Maximum moment capacity of the section under an axial load of P.
M_{pr} = Maximum probable moment capacity of the section under an axial load of P
M_{wcp} = Moment to be transferred by fillet welds between connection plates and column flange
M_y = Yield moment
P = Axial load
P_{pd} = Design vertical force for column base connection
P_{rp} = Design vertical pull for the rib plate
P_u = Ultimate capacity of column under axial loading
P_y = Yield capacity of column under axial loading
Q_E = Design earthquake load prescribed by code
R = Overall strength modification factor
R_c = Strength reduction factor due to compactness
R_L = Strength reduction factor due to flexural-torsional buckling of the member
R_y = Overstrength factor due uncertainty in the estimation of yield strength
R_λ = Strength reduction factor due to slenderness of the member
r = Radius or gyration
s = Ratio of plastic modulus to elastic modulus of the section (shape factor)
T_{cf} = Yield capacity of column flange
T_{cp} = Yield capacity of vertical flange cover plate
T_{cp}^* = Yield capacity of vertical flange cover plate provided
T_d = Design pull force for the top half of the connection

T_{rp} = Design pull force for the rib plate

T_{rp}^* = Yield capacity of rib plate provided

T_{wcp} = Vertical force transferred by fillet welds between cover plates and column flange

t = Thickness

t_{cf} = Thickness of column flange

t_{cp} = Thickness of vertical flange cover plate

t_{cw} = Thickness of column web

t_{rp} = Thickness of the rib plate

t_{wcp} = Thickness of fillet weld between connection plates and column flange

t_{wrp} = Thickness of fillet weld between connection plates and rib plates

V = Shear force

V_p = Section plastic shear capacity using minimum specified yield strength

V_{pd} = Connection design shear

V_{pr} = Maximum probable shear capacity of the section under an axial load of P

V_y = Yield shear

V_1 = Shear in column corresponding to failure Mechanism I

V_2 = Shear in column corresponding to failure Mechanism II

Z_c = Plastic section modulus of the column

φ = Curvature of the section

λ_c = Global slenderness parameter for member

λ_p = Limiting slenderness parameter for compact section

λ_r = Limiting slenderness parameter for non-compact section

σ_{xx} = Normal stress

τ_{xz} = Shear stress

τ_y = Minimum specified shear yield stress of steel = $F_y/\sqrt{3}$, first yield shear stress corresponding to the state of pure shear

Ω_o = System overstrength factor